The Journal of Pathology: Clinical Research
J Pathol Clin Res November 2022; **8:** 567–578
Published online 16 September 2022 in Wiley Online Library (wileyonlinelibrary.com). DOI: 10.1002/cjp2.295

ORIGINAL ARTICLE

Cellular dissociation grading on biopsies of pulmonary squamous cell carcinoma provides prognostic information across all stages and is congruent with resection specimen grading

Moritz Jesinghaus[1,2†], Melanie Boxberg[2,3†], Maxime Schmitt[1,2], Mark Kriegsmann[4,5], Alexander Harms[4], Corinna Lang[2], Thomas Muley[5,6,7], Hauke Winter[5,6,8], Katharina Kriegsmann[9], Arne Warth[10], Albrecht Stenzinger[4,5], Carsten Denkert[1], Hans Hoffmann[11], Seyer Safi[11] and Wilko Weichert[2,12,13*]

[1]*Institute of Pathology, University Hospital Marburg, Marburg, Germany*
[2]*Institute of Pathology, Technical University Munich, Munich, Germany*
[3]*Institute of Pathology Munich North, Munich, Germany*
[4]*Institute of Pathology, University Hospital Heidelberg, Heidelberg, Germany*
[5]*Member of the German Center for Lung Research (DZL), Heidelberg, Germany*
[6]*Translational Lung Research Center Heidelberg (TLRC-H), Heidelberg, Germany*
[7]*Translational Research Unit, Thoraxklinik at Heidelberg University Hospital, Heidelberg, Germany*
[8]*Department of Thoracic Surgery, Thoraxklinik at Heidelberg University Hospital, Heidelberg, Germany*
[9]*Department of Hematology, Oncology and Rheumatology, University Hospital Heidelberg, Heidelberg, Germany*
[10]*Institute of Pathology, Wetzlar, Germany*
[11]*Department of Thoracic Surgery, Klinikum Rechts der Isar (MRI), Munich, Germany*
[12]*German Cancer Consortium (DKTK), Partner Site Munich, Heidelberg, Germany*
[13]*Comprehensive Cancer Center Munich (CCCM), Munich, Germany*

**Correspondence to: Wilko Weichert, Institute of Pathology, Technical University Munich, Trogerstr. 18, 81675 Munich, Germany. E-mail: wilko.weichert@tum.de*

†These authors contributed equally to this work.

Abstract

Grading of squamous cell carcinomas (SCCs) based on tumour budding and cell nest size has been termed cellular dissociation grading (CDG) and was suggested as a robust outcome predictor when assessed in biopsies and resections of various extrapulmonary SCCs. In pulmonary SCC (pSCC), this has so far been shown only for resected cancers. As most lung cancers are inoperable, it is of utmost importance to clarify whether the prognostic impact of CDG is retained in the biopsy setting. Two independent pSCC biopsy cohorts from Munich ($n = 134$, non-resected) and Heidelberg ($n = 135$, resected) were assessed. Tumour budding and cell nest size measures were assembled into the three-tiered CDG system (G1–G3). Data were correlated with clinicopathological parameters and overall- (OS), disease-specific- (DSS), and disease-free survival (DFS). Interobserver variability and concordance between biopsy and resection specimen were also investigated. CDG was highly congruent between biopsy and resection specimens ($\kappa = 0.77$, $p < 0.001$). In both pSCC cohorts, biopsy-derived CDG strongly impacted on OS, DSS, and DFS (e.g. DFS: $p < 0.001$). In multivariate survival analyses, CDG remained a stage independent predictor of survival in both cohorts (DFS: $p < 0.001$ respectively; hazard ratio Munich cohort: CDG-G2: 4.31, CDG-G3; 5.14; Heidelberg cohort: CDG-G2: 5.87, CDG-G3: 9.07). Interobserver agreement for CDG was almost perfect ($\kappa = 0.84$, $p < 0.001$). We conclude that assessment of CDG based on tumour budding and cell nest size is feasible on pSCC biopsies and harbours stage independent prognostic information in resectable as well as non-resectable pSCC. Integration of this grading approach into clinicopathological routine should be considered.

Keywords: squamous cell carcinoma; cellular dissociation grading; lung; biopsy; tumour budding; cell nest size

Received 1 June 2022; Revised 8 August 2022; Accepted 31 August 2022

Conflicts of interest statement: WW has attended Advisory Boards and served as a speaker for Roche, MSD, BMS, AstraZeneca, Pfizer, Merck, Lilly, Boehringer, Novartis, Takeda, Bayer, Amgen, Astellas, Eisai, Johnson & Johnson, Janssen, Illumina, Siemens, Agilent, ADC, GSK and Molecular Health. WW has received research funding from Roche, MSD, BMS and AstraZeneca. CD has consulting or advisory roles with MSD Oncology, Daiichi Sankyo, Molecular Health, AstraZeneca, Merck,

Roche and Lilly, research funding from Myriad Genetics and Roche, and stock and other ownership interests in Sividon Diagnostics (until 2016). CD has patents, royalties and other intellectual property in VMScope digital pathology software, patent applications WO2015114146A1 and WO2010076322A1 – therapy response and patent application WO2020109570A1 – cancer immunotherapy. AS has memberships of Advisory Board/Speaker's Bureaus for AGCT, Aignostics, Astra Zeneca, Bayer, BMS, Eli Lilly, Illumina, Incyte, Janssen, MSD, Novartis, Pfizer, Roche, Seattle Genetics, Takeda and ThermoFisher, and grants from Bayer, BMS, Chugai, Incyte. MK declares consulting/oral presentations for GSK, Boehringer-Ingelheim. SS declared lecture fees from Coliquio GmbH and grants from the Else Kröner Fresenius Stiftung. All other authors declared no conflicts of interest.

Introduction

Lung cancer is the leading cause of cancer-related death in the western world. Pulmonary squamous cell carcinoma (pSCC) is the second most prevalent histologic subtype of lung cancer, comprising approximately 20% of all cases [1]. Tremendous progress has been made in the battle against lung cancer based on the molecular selection of patients for targeted treatments [2]; however, it has been the patients with pulmonary adenocarcinoma who have been benefitting the most from these developments [3,4].

Despite the fact, that broad molecular characterisation has been introduced to the clinical handling of lung cancer patients [5], the last decade has also brought a resurge of morphologic parameters as useful tools to predict patient outcomes and even responses to conventional chemotherapeutics [6–8]. But again, these developments took place mainly in lung adenocarcinomas.

For pSCC however, pathologists find themselves in a different situation, as currently morphology-based predictors for patients' outcome are nearly irrelevant for clinical decision making. The commonly proposed grading algorithm for squamous cell carcinomas (SCCs) – based on keratinisation, nuclear atypia, and mitotic rate – that is used commonly to grade pulmonary and extrapulmonary SCCs, shows high interobserver variability and – at best – is of minimal prognostic relevance, which is probably why it is no longer even mentioned in the pSCC chapter of the current WHO classification of thoracic tumours [9,10].

Recently, tumour budding and cell nest size, two parameters that quantitatively and qualitatively describe the extent of cellular dissociation, have been introduced as potentially relevant morphologic grading factors that might show a higher correlation with patients' outcome than conventional grading approaches. In previous studies, the combination of these cellular dissociation parameters was used to develop a novel grading approach that was consequently termed 'cellular dissociation grading' (CDG). In those studies, cellular dissociation based grading outperformed established grading algorithms in resected SCCs (and adenocarcinomas) from various anatomical sites, including oesophageal [11–14], head and neck [15,16], and cervical SCCs [17–19]. For head and neck and oesophageal SCC, it has already been confirmed that CDG is also feasible and clinically meaningful when assessed in pre-therapeutic biopsies of these tumours [14,16].

Based on early works by Kadota *et al* [10], our group – and others' – were able to show that cellular dissociation based grading also holds strong predictive power in resected pSCC [9,10,20,21]. However, for pSCC it remains entirely unclear whether the CDG approach is transferable to the biopsy situation, and if so whether CDG derived from pSCC biopsies is congruent between different observers and mirrors the grade derived from consecutive resection specimens. The latter is obviously specifically important, since it has to be answered whether an assessment on tiny biopsy samples is able to recapitulate the extent of cellular dissociation of a large, usually non-resected [22] lung neoplasm. In addition, it is yet entirely unclear whether CDG holds prognostic power in the clinical scenario of stage IV pSCC.

To address these questions, our study assessed tumour budding and cell nest size in pSCC biopsies from two independent and clinically distinct cohorts (non-resected versus resected). We investigated the prognostic value of the resulting CDG approach in the biopsy scenario of pSCC and compared the results with data previously obtained from consecutive resection specimen.

Materials and methods

Patient cohorts

This study was approved by the local ethical committees of the University Hospital Heidelberg (reference: 301/2001) and of the University Hospital Rechts der Isar of the Technical University of Munich (reference number: 2022-119-S).

Two independent pSCC biopsy cohorts were investigated. The first pSCC biopsy cohort (Munich cohort) comprised 134 non-resected cases treated between 1999 and 2018. The median age of patients was 68 years, 104 (77.6%) patients were male, 30 (22.4%) were female. As these patients were not surgically treated, only clinical staging data were available: 16 (11.5%)

pSCCs were clinical stage I, stage II was diagnosed in 5 cases (3.7%), stage III was present in 29 (21.7%) cases, and stage IV was evident in 84 (62.7%) cases.

The second cohort was a subcohort of 135 patients with operable pSCC from the University Hospital Heidelberg, from which pre-therapeutic biopsies were available (Heidelberg cohort, patients treated between 2005 and 2010). These patients were part of a much larger collective of resected pSCCs, which were investigated regarding tumour budding and cell nest size in a previous study [21]. Therefore, all cases from the Heidelberg cohort had available data from consecutive resection specimen that could be compared to the newly generated data from the preoperative biopsies that were investigated in this study. The median age of patients in this cohort was 65 years. One-hundred and fifteen (85.2%) patients were male, 20 (14.8%) were female: 39 (28.9%) cases of this cohort were pathological UICC stage I, 19 (14.1%) were UICC stage II, 71 (52.6%) were UICC stage III, and 6 (4.4%) were UICC stage IV. Compared to one another, the two cohorts showed a similar ratio between males and females, a comparable median age as well as a similar distribution of keratinising and non-keratinising carcinomas (p = n.s.). Although clinical and pathological stage cannot exactly be compared and are only an approximation of one another, a massive enrichment of stage IV patients compared to the Heidelberg cohort was evident in the Munich cohort ($p < 0.001$, clinical versus pathological stage). Detailed clinicopathological characteristics including survival associations are given in Table 1 (Munich cohort) and Table 2 (Heidelberg cohort).

Histopathological evaluation

Three experienced pathologists (MJ, MB, and WW) who were blinded to clinicopathological data were involved in the evaluation of H&E-stained slides of pSCC biopsy specimens. MJ performed the initial evaluation of all biopsies. MB blindly reassessed cases initially evaluated by MJ to test interobserver variability. For discrepant cases, WW was called in as a reference pathologist in order to reach a consensus. All section levels on the available slides were taken into account. Only diagnostic biopsies harbouring clearly invasive carcinomas were considered, cases that only showed minimal invasive cancer surrounding an *in situ* lesion were excluded. An Olympus BX46 microscope (Olympus, Shinjuku, Tokyo, Japan) with a field diameter of 0.55 mm (0.24 mm^2) was used. Resection specimens from the Heidelberg cohort had previously been evaluated in an independent study [21].

Tumour budding and cell nest size and the resulting CDG were quantified as described previously (Figure 1 and Table 3) [14]. In brief, tumour budding was used as a quantitative parameter to determine the extent of dissociative growth and defined as the presence of small, stroma invasive tumour complexes of fewer than five tumour cells. Tumour buds were counted in one high-power-field (HPF) in biopsies in the area showing maximal budding activity at a scanning magnification. The presence of 1–4 tumour buds in one HPF was defined as a low budding activity. Tumours with ≥5 buds in one HPF were assigned to the high budding activity subgroup. Cell nest size was assessed as a qualitative parameter for the maximal capability of dissociative growth of a given tumour. Tumour cell nests were classified according to the size of the smallest invasive cell nest as follows: >15 tumour cells = large nests, 5–15 tumour cells = intermediate size nests, 2–4 tumour cells = small nests, and discohesive tumour cells without nested architecture = single-cell invasion. The criteria applied for budding activity and cell nest size evaluation were similar to already published algorithms for the evaluation of *CDG* in biopsies and resection specimen [11,15,16,21]. A scoring system for both the extent of tumour budding activity (1 = no budding activity; 2 = low budding activity; 3 = high budding activity) and cell nest size (1 = large cell nests; 2 = intermediate cell nests; 3 = small cell nests; 4 = single-cell invasion) was used in order to generate a composite CDG score. Similarly to the cutoffs used in previous studies from our group [11,15,16,21], both scores for tumour budding and cell nest size were incorporated into a sum score ranging from 2 to 7, raw scores were used to classify cancers of being not dissociative (CDG G1; sum scores 2–3), moderately dissociative (CDG G2; sum scores 4–6), and highly dissociative (CDG G3; sum score 7). The detailed algorithm to determine the CDG is depicted in Table 3.

Assessment of interobserver variability

A total of 90 cases (randomly selected from both cohorts) were independently evaluated by two experienced pathologists (MJ and MB) to assess interobserver variability (see above).

Statistics

Associations of morphological characteristics with clinicopathological parameters were calculated with χ^2 tests and Fisher's exact test. Survival probabilities were plotted with the Kaplan–Meier method, a log-rank test was used to probe the significance of differences. Multivariate survival analysis was performed with the Cox proportional hazard model. P values ≤0.05 were considered significant. Interobserver variability was analysed by using κ

Table 1. Clinicopathological characteristics of the Munich cohort and their association with patient survival

	Overall *n* (%)	Mean OS (SE) (months)	*P* value	Mean DSS (SE) (months)	*P* value	Mean DFS (SE) (months)	*P* value
Age			0.359		0.529		0.668
Below median	62 (46.3%)	17.26 (2.3)		17.54 (2.4)		15.11 (2.2)	
Above median	72 (53.7%)	14.78 (2.0)		16.15 (2.2)		14.44 (2.1)	
Sex			0.698		0.891		0.828
Male	104 (77.6%)	15.87 (1.7)		16.95 (1.9)		14.99 (1.8)	
Female	30 (22.4%)	16.08 (3.1)		16.08 (3.1)		13.61 (3.1)	
cT (not all data available)			**0.003**		**0.003**		**0.006**
1	5 (7.0%)	51.16 (11.2)		51.16 (7.9)		50.80 (8.2)	
2	25 (35.3%)	20.70 (3.4)		21.44 (3.7)		18.02 (3.5)	
3	17 (23.9%)	16.63 (3.5)		16.63 (3.5)		13.89 (3.5)	
4	24 (33.8%)	12.19 (2.2)		12.19 (2.2)		11.55 (2.4)	
cN (not all data available)			0.106		**0.079**		**0.022**
0	29 (39.7%)	26.31 (4.2)		27.27 (4.4)		25.46 (4.3)	
1	8 (11.0%)	16.69 (6.5)		16.69 (6.5)		11.88 (4.0)	
2	22 (30.1%)	15.65 (2.1)		15.65 (2.1)		11.92 (1.9)	
3	14 (19.2%)	12.29 (2.6)		12.29 (2.6)		9.25 (1.5)	
cM			0.050		0.061		**0.021**
0	51 (38.1%)	19.98 (2.8)		20.62 (2.9)		19.01 (2.9)	
1	83 (61.9%)	13.44 (1.7)		14.40 (1.8)		11.89 (1.6)	
Clinical stage			**0.025**		**0.015**		**0.014**
1	16 (11.9%)	31.44 (5.9)		33.28 (6.3)		30.52 (6.2)	
2	5 (3.7%)	18.38 (9.7)		18.38 (9.7)		16.72 (9.8)	
3	29 (21.7%)	13.37 (2.0)		13.37 (2.0)		12.45 (2.1)	
4	84 (62.7%)	13.36 (1.7)		14.30 (1.8)		11.82 (1.6)	
Tumour budding			**0.002**		**0.002**		**<0.001**
0	14 (10.5%)	53.01 (13.1)		58.84 (13.3)		56.54 (13.0)	
1–4	68 (50.7%)	15.15 (2.2)		16.13 (2.5)		15.48 (2.6)	
≥5	52 (38.8%)	15.14 (3.4)		16.22 (3.6)		13.08 (3.1)	
Cell nest size			**0.002**		**0.002**		**0.001**
>15	5 (3.7%)	59.48 (25.6)		59.48 (25.6)		53.33 (21.9)	
5–15	9 (6.7%)	47.29 (15.6)		55.14 (16.7)		54.38 (16.8)	
2–4	41 (30.6%)	18.78 (3.6)		20.72 (4.4)		18.65 (4.2)	
Single cell invasion	79 (59.0%)	13.68 (2.4)		14.31 (2.5)		12.42 (2.9)	
CDG biopsy			**0.001**		**0.001**		**<0.001**
CDG-G1	14 (10.4%)	53.00 (13.10)		58.84 (13.28)		56.54 (12.98)	
CDG-G2	73 (54.5%)	16.57 (2.69)		18.02 (3.21)		17.43 (3.31)	
CDG-G3	47 (35.1%)	13.30 (2.89)		14.34 (3.11)		10.95 (2.37)	

P values in bold are statistically significant.

statistics, the interpretation of kappa-values was guided by the classification proposed by Landis and Koch [23] ($\kappa < 0$: less than chance agreement, $\kappa = 0.01$–0.20: slight agreement, $\kappa = 0.21$–0.40: fair agreement, $\kappa = 0.41$–0.60: moderate agreement, $\kappa = 0.61$–0.80: substantial agreement, $\kappa = 0.81$–0.99: almost perfect agreement).

Results

Distribution of tumour budding/cell nest size and the resulting CDG within both biopsy cohorts

In the Munich cohort (Table 1), 14 (10.5%) out of 134 biopsies showed no tumour budding, while 68 (50.7%) cases showed intermediate tumour budding activity. A high tumour budding activity was noted in 52 (38.8%) pSCC biopsies. Five (3.7%) cases showed large cell nests of more than 15 cells as their smallest cell nest size, 9 (6.9%) biopsies showed intermediate cell nests, a small cell nest size (minimal size of 2–4 cells) was noted in 41 (30.6%) biopsies. Single cell invasion was present in 79 (59.0%) cases. The combination of both parameters (Table 3) resulted in 14 (10.4%) CDG-G1 (10%), 73 (54.5%) CDG-G2, and 47 (35.1%) CDG-G3 cases.

In the resected Heidelberg cohort (Table 2), the number of cases with increased tumour budding and decreased cell nest sizes was considerably lower. Fifty-six (41.5%) out of 135 biopsies showed no tumour budding, 55 (40.7%) cases showed intermediate tumour

Table 2. Clinicopathological characteristics of the Heidelberg cohort and their association with patient survival

	Overall *n* (%)	Mean OS (SE) (months)	*P* value	Mean DSS (SE) (months)	*P* value	Mean DFS (SE) (months)	*P* value
Age			0.136		0.162		0.500
Below median	65 (48.1%)	56.09 (2.9)		56.85 (2.9)		48.23 (3.5)	
Above median	70 (51.9%)	46.32 (3.0)		47.45 (2.9)		42.83 (3.2)	
Sex			0.126		0.060		0.379
Male	115 (85.2%)	50.32 (2.5)		51.08 (2.5)		45.45 (2.7)	
Female	20 (14.8%)	39.68 (2.2)		41.33 (1.5)		34.23 (3.4)	
pT			**0.024**		**0.009**		**0.028**
1a	20 (14.8%)	58.23 (5.2)		58.23 (5.2)		55.00 (5.8)	
1b	17 (12.6%)	43.62 (5.4)		43.62 (5.4)		33.28 (5.8)	
2a	41 (30.4%)	45.07 (2.1)		46.86 (1.8)		40.86 (2.6)	
2b	23 (17.0%)	38.87 (3.3)		38.87 (3.3)		33.29 (3.9)	
3	27 (20.0%)	32.33 (2.6)		33.13 (2.6)		29.03 (3.0)	
4	7 (5.2%)	23.14 (3.1)		23.14 (3.1)		17.23 (4.4)	
pN			0.211		0.087		0.210
0	64 (47.4%)	52.78 (3.1)		52.78 (3.1)		45.86 (3.6)	
1	50 (37.0%)	44.10 (2.5)		46.31 (2.3)		40.88 (2.8)	
2	21 (15.6%)	30.47(2.8)		30.47 (2.8)		25.87 (3.3)	
pM			**<0.001**		**<0.001**		**<0.001**
0	129 (95.6%)	54.05 (2.2)		55.15 (2.2)		48.32 (2.5)	
1a	6 (4.4%)	17.00 (7.0)		16.99 (7.0)		6.28 (1.4)	
Pathological UICC stage			**<0.001**		**<0.001**		**<0.001**
1	39 (28.9%)	59.18 (3.3)		59.18 (3.3)		51.48 (4.2)	
2	19 (14.1%)	48.22 (4.6)		48.22 (4.6)		39.37 (5.0)	
3	71 (52.6%)	42.17 (2.2)		43.63 (2.1)		38.17 (2.5)	
4	6 (4.4%)	16.99 (7.0)		16.99 (7.0)		6.38 (1.4)	
Tumour budding biopsy			**<0.001**		**<0.001**		**<0.001**
0	56 (41.5%)	63.89 (2.0)		64.86 (1.8)		60.65 (2.6)	
1–4	55 (40.7%)	45.38 (3.5)		46.09 (3.5)		37.87 (3.8)	
≥5	24 (17.8%)	33.83 (4.2)		34.91 (4.3)		25.68 (4.1)	
Cell nest size biopsy			**<0.001**		**<0.001**		**<0.001**
>15	21 (15.6%)	66.07 (1.4)		66.07 (1.4)		62.47 (3.7)	
5–15	36 (26.7%)	55.52 (3.0)		56.83 (2.8)		53.75 (3.4)	
2–4	31 (23.0%)	50.38 (3.4)		51.82 (3.2)		42.00 (4.1)	
Single cell invasion	47 (34.8%)	35.13 (2.3)		35.76 (3.8)		30.05 (4.1)	
CDG biopsy			**<0.001**		**<0.001**		**<0.001**
CDG-G1	56 (41.5%)	63.89 (2.0)		64.86 (1.8)		60.65 (2.6)	
CDG-G2	57 (42.2%)	45.36 (3.4)		46.79 (3.4)		38.16 (3.7)	
CDG-G3	22 (16.3%)	33.32 (4.6)		33.32 (4.6)		24.15 (4.3)	
CDG resection			**<0.001**		**<0.001**		**<0.001**
CDG-G1	60 (44.4%)	63.07 (2.1)		63.97 (1.9)		56.28 (3.2)	
CDG-G2	55 (40.7%)	46.82 (3.4)		48.31 (3.4)		42.59 (3.8)	
CDG-G3	20 (14.8%)	31.62 (5.0)		31.62 (5.0)		22.24 (5.0)	

P values in bold are statistically significant.

budding (41%). A high tumour budding activity was noted in 24 (17.8%) pSCC biopsies. Twenty-one (15.6%) cases harboured large cell nests, 36 (26.7%) cases had intermediate sized cell nests (27%), a small cell nest size (minimal size of 2–4 cells) was noted in 31 (23%) biopsies. Single cell invasion was present in 47 (34.8%) cases. The combination of both parameters (Table 3) resulted in 56 (41.5%) CDG-G1, 57 (42.2%) CDG-G2, and 22 (16.3%) CDG-G3 cases.

When we compared the distribution of CDG-grades between both cohorts, we observed a significantly higher frequency of highly dissociative CDG-G3 neoplasms (35.1% [Munich] versus 16.3% [Heidelberg]; $p < 0.001$) and a significantly lower frequency of non-dissociative CDG-G1 tumours in the non-resected Munich cohort compared to the resected Heidelberg cohort (10.4% [Munich] versus 41.5% [Heidelberg]; $p < 0.001$).

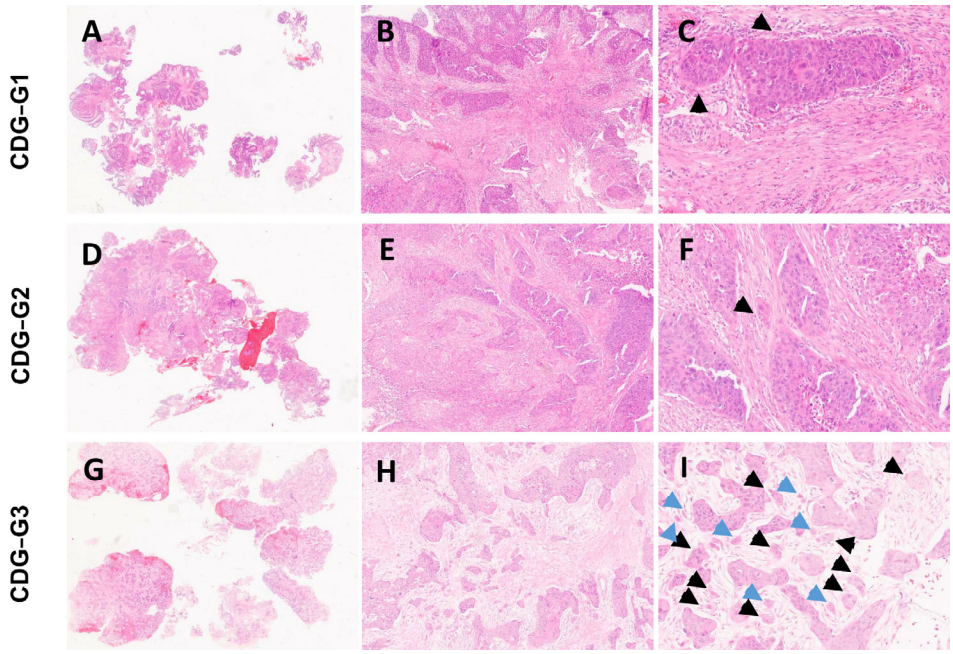

Figure 1. Histopathology of pSCC biopsies with different CDGs. (A–C) (A: ×1.25) Scanning magnification from a biopsy of a CDG-G1 invasive pSCC showing a neoplasm without tumour budding consisting of (B: ×10) very large cell-nests of more than 15 cells (C: ×40, arrows mark the large cell-nests). (D–F) (D: ×1.25) Scanning magnification from a biopsy of a CDG-G2 invasive pSCC with moderate dissociative growth featuring moderate tumour budding with small cell nests but no single cell invasion. (E: ×10) While also larger cell nests are seen, there are (F: ×40, arrow) few small invasive cell nests that consist of less than five cells. No single-cell invasion was noted. (G–I) (G: ×1.25) Scanning magnification from a biopsy of a CDG-G3 pSCC with (H: ×10) highly dissociative growth. The tumour shows high tumour budding with numerous invasive clusters of less than 2–4 cells (black arrows) and (I: ×40) numerous invasive single cells (blue arrows).

Correlation of tumour budding/cell nest size and the resulting CDG with clinicopathological parameters

In the Munich cohort, CDG ($p = 0.04$) and cell nest size ($p = 0.007$) were associated with higher clinical stages, while tumour budding only trended towards higher clinical stages ($p = 0.067$) without reaching statistical significance. No association of any of the parameters with age was noted.

In the Heidelberg cohort, pathological UICC stage was not significantly associated with tumour budding and cell nest size. The derived CDG trended to be higher in high tumour stages ($p = 0.075$), but this association did also not reach statistical significance. No correlation of any of the parameters with age and sex was observed.

Table 3. Algorithm for the calculation of CDG on pSCC biopsies

Algorithm for the assembly of CDG for biopsy specimens of pSCC	Score
Tumour budding/1 HPF	
No tumour budding	1
1–4 tumour buds detectable	2
5 or more tumour buds detectable	3
Smallest cell nest size	
>15 cells	1
5–15 cells	2
2–4 cells	3
Single cell invasion	4
CDG	
CDG-G1 (well differentiated)	2–3
CDG-G2 (moderately differentiated)	4–6
CDG-G3 (poorly differentiated)	7

Correlation of tumour budding/cell nest size and the resulting CDG assessed on pSCC biopsies with survival parameters

Both cellular dissociation parameters, tumour budding as well as cell nest size as assessed on pSCC biopsies were significant survival predictors for overall (OS), disease-specific (DSS), and disease-free survival (DFS) in the Munich cohort as well as in the Heidelberg cohort (see Table 1 [Munich] and supplementary material, Figure S1, and Table 2 [Heidelberg] and supplementary material, Figure S2).

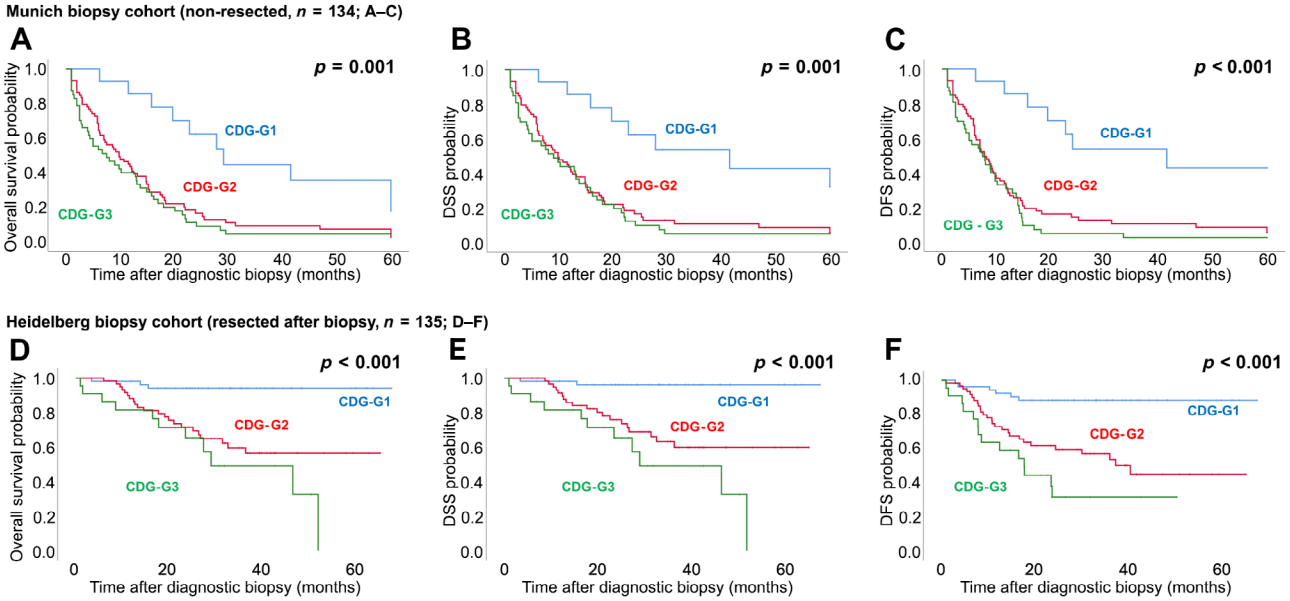

Figure 2. Impact of CDG derived from pSCC biopsies on OS, DSS, and DFS probability in (A–C) the Munich cohort and (D–F) in the Heidelberg cohort.

In univariate survival analyses of the Munich cohort (Table 1, Figure 2), the CDG derived from a combination of tumour budding and cell nest size (Table 1) was strongly associated with OS ($p = 0.001$; CDG-G1: 53.00 months versus CDG-G2: 16.57 months versus CDG-G3 13.30 months), DSS ($p = 0.001$; CDG-G1: 58.84 months versus CDG-G2: 18.02 months versus CDG-G3: 14.34 months), and DFS ($p < 0.001$; CDG-G1: 56.54 months versus CDG-G2: 17.43 months versus CDG-G3: 10.95 months). In multivariate analyses of the Munich cohort (Cox-regression) including CDG, age, gender, and clinical stage, CDG remained a stage independent prognosticator (DFS: $p < 0.001$, hazard ratio CDG-G2: 4.31, hazard ratio CDG-G3: 5.14, Table 4; DSS: $p = 0.001$, hazard ratio CDG-G2: 2.94, hazard ratio CDG-G3: 3.15, data not shown; OS: $p = 0.002$, hazard ratio CDG-G2: 3.34, hazard ratio CDG-G3: 3.41, data not shown).

As expected, and previously published [21], CDG as extracted from resection specimens in the Heidelberg cohort was a survival predictor for OS, DSS, and DFS (Table 2, Figure 3) in univariate analyses ($p < 0.001$ for all comparisons).

Table 4. Multivariate survival analysis for disease-free survival (Munich cohort)

	HR (DFS)	Lower CI (95%)	Upper CI (95%)	*P* value
CDG on biopsy				<0.001
CDG-G1	1.00			
CDG-G2	4.31	1.93	9.6	
CDG-G3	5.14	2.25	11.72	
Gender				0.50
Male	1.00			
Female	0.85	0.54	1.34	
Age group				0.98
Median and above	1.00			
Below median	0.96	0.68	1.44	
Clinical UICC stage				**0.004**
Stage I	1.00			
Stage II	1.51	0.47	4.84	
Stage III	2.02	0.97	4.21	
Stage IV	2.62	1.35	5.06	

P values in bold are statistically significant.

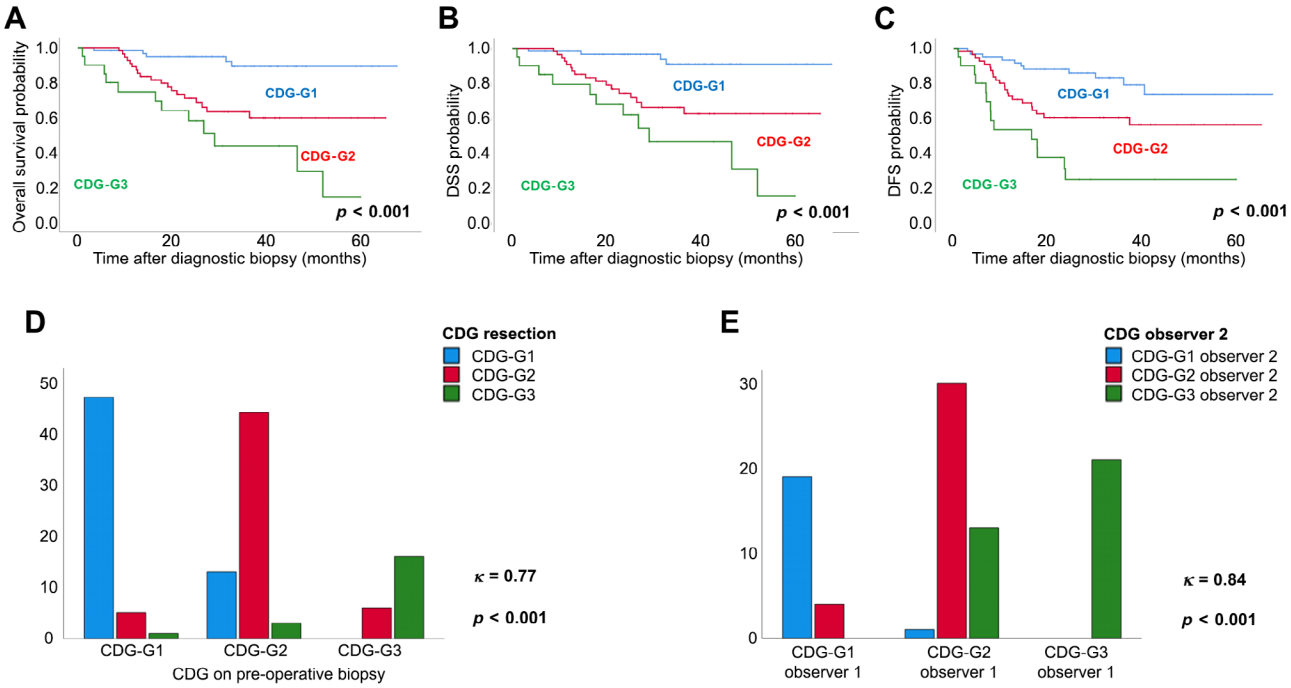

Figure 3. (A–C) Impact of CDG derived from resection specimens on OS, DSS, and DFS probability in the Heidelberg cohort as well as concordance of (D) the CDG between biopsies and resections and (E) between different observers.

CDG as assessed on biopsies in the resected Heidelberg cohort was also strongly associated with OS ($p < 0.001$; CDG-G1: 63.89 months versus CDG-G2: 45.36 months versus CDG-G3: 33.32 months), DSS ($p < 0.001$; CDG-G1: 64.86 months versus CDG-G2: 46.79 months versus CDG-G3: 33.32 months), and DFS ($p < 0.001$; CDG-G1: 60.65 months versus CDG-G2: 38.16 months versus CDG-G3: 24.15 months) (Table 2, Figure 2). In multivariate analyses of the Heidelberg cohort (Cox-regression) including biopsy derived CDG, age, gender, and clinical stage, the biopsy derived CDG remained a stage independent prognosticator (DFS: $p < 0.001$, hazard ratio CDG-G2: 5.87, hazard ratio CDG-G3: 9.07, Table 5; DSS: $p < 0.001$, hazard ratio CDG-G2: 8.04, hazard ratio CDG-G3: 9.83, data not shown; OS: $p = 0.002$, hazard ratio CDG-G2: 11.36, hazard ratio CDG-G3: 14.92, data not shown).

Table 5. Multivariate survival analysis for disease-free survival (Heidelberg cohort)

	HR (DFS)	Lower CI (95%)	Upper CI (95%)	*P* value
CDG on biopsy				<0.001
CDG-G1	1.00			
CDG-G2	5.87	2.38	14.45	
CDG-G3	9.07	3.32	24.80	
Gender				0.27
Male	1.00			
Female	0.58	0.22	1.53	
Age group				0.87
Median and above	1.00			
Below median	0.94	0.50	1.79	
Pathological UICC stage				**<0.001**
Stage I	1.00			
Stage II	1.88	0.67	5.21	
Stage III	1.10	0.50	2.41	
Stage IV	18.42	4.28	79.14	

P values in bold are statistically significant.

Concordance of tumour budding/cell nest size and the resulting CDG between biopsies and resections

We compared the congruency of the CDG derived from biopsies with those from resection specimens (Heidelberg cohort) and observed a substantial concordance between resections and previous biopsies ($\kappa = 0.77$, $p < 0.001$, Figure 3). Of the 53 pSCCs that were classified as CDG-G1 on biopsy, 47 were also classified CDG-G1 on the resection, while only 5 tumours were allocated to the post-operative CDG-G2 and only 1 neoplasm was allocated to the post-operative CDG-G3 category. Of the 60 CDG-G2 pSCCs on biopsy, 44 were also classified CDG-G2 on the resection, while 13 were CDG-G1 and 3 were CDG-G3 on the resection specimen. Of the 22 CDG-G3 pSCCs on biopsy, 16 were concordantly CDG-G3 on the resection, 6 were diagnosed as CDG-G2 on the resection.

Interobserver variability of tumour budding/cell nest size and the resulting CDG

Cases from both cohorts (Heidelberg cohort: $n = 50$, Munich cohort: $n = 40$) were consecutively and independently evaluated by two pathologists to assess interobserver variability. All assessments showed substantial interobserver agreement for both tumour budding ($\kappa = 0.75$, $p < 0.001$, data not shown) and cell nest size ($\kappa = 0.63$, $p < 0.001$, data not shown). This resulted in an almost perfect concordance of the CDG ($\kappa = 0.84$, $p < 0.001$; Figure 3). Only six cases were classified discordantly, in none of the cases was a deviation of more than one grade category noted. Of the 22 cases diagnosed as CDG-G1 by the main observer, 19 were similarly classified by the second pathologist, while 3 of those neoplasms were diagnosed as CDG-G2 by the second observer. The main observer diagnosed 45 tumours as CDG-G2, which were also diagnosed as CDG-G2 by the second pathologist in 40 cases (CDG-G1, $n = 2$; CDG-G3, $n = 3$). Of the 23 cases allocated to the CDG-G3 category by the main observer, only 1 biopsy was classified differently by the second pathologist (CDG-G2).

Discussion

Histopathological grading has relevant impact on patient management in a variety of tumour entities including breast cancer, prostate cancer, colorectal cancer, and sarcomas, just to mention a few [24–26]. In stark contrast, the WHO endorsed grading system for SCCs of the diverse anatomic sites throughout the body, which is based on the evaluation of nuclear pleomorphism, degree of keratinisation, and mitotic activity, is literally irrelevant for clinical decision making. This is due to the fact, that this grading approach has – at best – minimal prognostic power [12,15,17,21] and is known to show substantial interobserver variability [27].

In order to address the lack of a clinically relevant grading approach in these tumour entities, a variety of different groups, including ours, independently explored alternative algorithms for histopathological grading of SCCs. Examples of alternative grading algorithms proposed for SCCs are the malignancy grading of invasive margins, the tumour budding, and depth of invasion model or the histological risk model [28–30], which are not suitable for biopsies as they are either only applicable at the invasive front or combine histopathological parameters that describe the tumour architecture with non-architectural parameters (e.g. depth of invasion, perineural invasion, inflammatory response, etc).

In our view, the currently most promising alternative approach in this regard focuses on a quantification of the maximal capacity of dissociative growth of a given cancer and combines the *quantitative* cellular dissociation parameter 'tumour budding' with the *qualitative* cellular dissociation parameter 'cell nest size' to a new SCC grading scheme, that has consequently been termed Cellular Dissociation Grading (CDG).

CDG has been shown to be highly predictive of patient survival when assessed on resection specimen in a variety of SCC from different anatomic sites including head and neck, oesophagus, and cervix [11–13,15,17,31]. Additional studies on head and neck as well as oesophageal SCCs suggested an excellent transferability to the pretherapeutic biopsy situation at these sites [14,16].

Likewise, for pSCC, Kadota *et al* as well as our group were able to demonstrate that grading based on cellular dissociation parameters is a strong predictor of patient survival and relapse when assessed in resection specimens of pSCC [10,21]. However, for pSCC it remained entirely unclear, whether the CDG approach is transferable to diagnostic pSCC biopsies and especially, if the prognostic impact is retained in advanced, non-operable pSCCs.

Filling this knowledge gap, our data from two pSCC cohorts show that CDG derived from pSCC biopsies allows for an excellent demarcation of patient survival and relapse, which is also retained in multivariate analyses including tumour stage.

Although CDG generally worked fine with respect to patient stratification in both cohorts, some obvious differences were observed. The mean survival was substantially shorter in the non-resected cohort from

Munich than in the resected Heidelberg cohort, as the latter strongly biased towards earlier stages when compared to the overall lung cancer population. Compared to the resected cohort from Heidelberg, we observed significantly higher levels of tumour budding and smaller cell nest sizes and thus higher CDG grades in the non-resectable cohort from Munich. This is not surprising from a biological point of view, since it is likely that tumours with an unfavourable biology – for which an increased cellular dissociation capacity is a reliable surrogate parameter – are more common in more advanced/non-resectable pSCC.

We observed a fine prognostic delineation between the three CDG biopsy grades in the resected cohort, which was comparable to the CDG based prognostic delineation which we obtained from the corresponding resection specimen. In the non-resected Munich cohort, however, we observed a strong prognostic separation for CDG-G1 pSCCs from all other pSCC, while survival differences were significantly less pronounced between CDG-G2 and CDG-G3 pSCC, which both showed dismal survival characteristics. Considering the fact, that a significant number of CDG-G2 tumours in this high stage cohort showed single cell invasion, but only showed intermediate tumour budding in the biopsies, it is possible that a considerable fraction of these tumours might show higher tumour budding activity in other parts of the tumour and would therefore be upgraded to CDG-G3 on a hypothetical resection specimen, which would be even more consistent with their highly aggressive clinical behaviour. Furthermore, if we consider that the three-tiered CDG system has been shown to be extremely prognostic in almost all other study cohorts [11–17,32] including our second cohort of resected pSCCs, we would not advocate introducing a two-stage CDG system especially for non-operable pSCC.

One factor which is also important for the use of morphology-based prognostic/predictive factors in patient management is how reliable a given classification can be done. Thus, interobserver variability must be known, before any implementation of such parameters into routine diagnostics. For grading based on cellular dissociation parameters there is already some data out there suggesting reproducibility, however, most of these data were obtained from resection specimen [32]. Here, we were able to show that even the supposedly more difficult evaluation on biopsies can be done with an almost perfect interobserver agreement [23].

One of the shortcomings of our work is that our analysis is retrospective in nature. However, to at least mitigate cohort bias, we included two entirely independent cohorts from different clinical centres in our project and could show that the effect of biopsy based CDG on prognosis was robust and reproducible. Another shortcoming is, that we did not include any treatment modalities (except from surgical resection) into our analysis. Although some information on postoperative adjuvant or first line palliative treatment was available in both cohorts, due to the fact that we included patients from a time span of more than two decades, treatments were too diverse to compile any meaningful groups with sufficient sample size from these data. In addition, given the timeline of case recruitment only very few patients received something else than conventional (radio)chemotherapy. Thus, it has to be determined in the future whether the specific prognostic impact of CDG somehow interacts with the administered adjuvant or palliative therapeutic regimens. This will be particularly interesting in the context of novel immune oncology approaches such as immune checkpoint inhibitor treatment, since it has been suggested that epithelial to mesenchymal transformation – for which both tumour budding and cell nest size are believed to be morphology-based surrogates [33,34] – significantly impacts on the response to immune checkpoint inhibitors [35] as it is associated with tremendous changes in the composition of the immune microenvironment [36].

Taken together, our study demonstrates that CDG based on tumour budding and cell nest size of pSCCs is feasible on diagnostic biopsy specimen and provides stage independent prognostic information. Thus, we believe that routine diagnostic evaluation of these parameters should be considered.

Acknowledgements

We acknowledge the iBio biomaterial bank of the Technical University Munich and the Biomaterialbank (BMBH) Heidelberg for technical support.

Author contributions statement

MJ, MB and WW designed this study and wrote the paper with assistance from all listed authors. Statistical analyses were performed by MJ, MB, CD, KK, MK and WW. All authors collected clinicopathological data. Histopathological analyses were performed by MJ, MM, AH, MK, AS and WW.

Data availability statement

All data relevant to this study are given in the main paper including figures, tables and supplementary files.

The tissue investigated for this study is archived in the Institute of Pathology of the Technical University of Munich and the Institute of Pathology of the University Hospital Heidelberg.

References

1. Barta JA, Powell CA, Wisnivesky JP. Global epidemiology of lung cancer. *Ann Glob Health* 2019; **85**: 8.
2. Herbst RS, Morgensztern D, Boshoff C. The biology and management of non-small cell lung cancer. *Nature* 2018; **553**: 446–454.
3. Reck M, Rabe KF. Precision diagnosis and treatment for advanced non-small-cell lung cancer. *N Engl J Med* 2017; **377**: 849–861.
4. Jordan EJ, Kim HR, Arcila ME, *et al*. Prospective comprehensive molecular characterization of lung adenocarcinomas for efficient patient matching to approved and emerging therapies. *Cancer Discov* 2017; **7**: 596–609.
5. Ettinger DS, Wood DE, Aisner DL, *et al*. Non-small cell lung cancer, version 5.2017, NCCN Clinical Practice Guidelines in Oncology. *J Natl Compr Cancer Netw* 2017; **15**: 504–535.
6. Shih AR, Mino-Kenudson M. Updates on spread through air spaces (STAS) in lung cancer. *Histopathology* 2020; **77**: 173–180.
7. Warth A, Muley T, Meister M, *et al*. The novel histologic International Association for the Study of Lung Cancer/American Thoracic Society/European Respiratory Society classification system of lung adenocarcinoma is a stage-independent predictor of survival. *J Clin Oncol* 2012; **30**: 1438–1446.
8. Travis WD, Brambilla E, Noguchi M, *et al*. International Association for the Study of Lung Cancer/American Thoracic Society/European Respiratory Society international multidisciplinary classification of lung adenocarcinoma. *J Thorac Oncol* 2011; **6**: 244–285.
9. Kadota K, Miyai Y, Katsuki N, *et al*. A grading system combining tumor budding and nuclear diameter predicts prognosis in resected lung squamous cell carcinoma. *Am J Surg Pathol* 2017; **41**: 750–760.
10. Kadota K, Nitadori J, Woo KM, *et al*. Comprehensive pathological analyses in lung squamous cell carcinoma: single cell invasion, nuclear diameter, and tumor budding are independent prognostic factors for worse outcomes. *J Thorac Oncol* 2014; **9**: 1126–1139.
11. Boxberg M, Kuhn PH, Reiser M, *et al*. Tumor budding and cell nest size are highly prognostic in laryngeal and hypopharyngeal squamous cell carcinoma: further evidence for a unified histopathologic grading system for squamous cell carcinomas of the upper aerodigestive tract. *Am J Surg Pathol* 2019; **43**: 303–313.
12. Jesinghaus M, Boxberg M, Konukiewitz B, *et al*. A novel grading system based on tumor budding and cell nest size is a strong predictor of patient outcome in esophageal squamous cell carcinoma. *Am J Surg Pathol* 2017; **41**: 1112–1120.
13. Jesinghaus M, Boxberg M, Wilhelm D, *et al*. Post-neoadjuvant cellular dissociation grading based on tumour budding and cell nest size is associated with therapy response and survival in oesophageal squamous cell carcinoma. *Br J Cancer* 2019; **121**: 1050–1057.
14. Jesinghaus M, Bruhl F, Steiger K, *et al*. Cellular dissociation grading based on the parameters tumor budding and cell nest size in pretherapeutic biopsy specimens allows for prognostic patient stratification in esophageal squamous cell carcinoma independent from clinical staging. *Am J Surg Pathol* 2019; **43**: 618–627.
15. Boxberg M, Jesinghaus M, Dorfner C, *et al*. Tumour budding activity and cell nest size determine patient outcome in oral squamous cell carcinoma: proposal for an adjusted grading system. *Histopathology* 2017; **70**: 1125–1137.
16. Jesinghaus M, Steiger K, Stogbauer F, *et al*. Pre-operative cellular dissociation grading in biopsies is highly predictive of post-operative tumour stage and patient outcome in head and neck squamous cell carcinoma. *Br J Cancer* 2020; **122**: 835–846.
17. Jesinghaus M, Strehl J, Boxberg M, *et al*. Introducing a novel highly prognostic grading scheme based on tumour budding and cell nest size for squamous cell carcinoma of the uterine cervix. *J Pathol Clin Res* 2018; **4**: 93–102.
18. Shi H, Ye L, Lu W, *et al*. Grading of endocervical adenocarcinoma: a novel prognostic system based on tumor budding and cell cluster size. *Mod Pathol* 2022; **35**: 524–532.
19. Zare SY, Aisagbonhi O, Hasteh F, *et al*. Independent validation of tumor budding activity and cell nest size as determinants of patient outcome in squamous cell carcinoma of the uterine cervix. *Am J Surg Pathol* 2020; **44**: 1151–1160.
20. Neppl C, Zlobec I, Schmid RA, *et al*. Validation of the International Tumor Budding Consensus Conference (ITBCC) 2016 recommendation in squamous cell carcinoma of the lung-a single-center analysis of 354 cases. *Mod Pathol* 2020; **33**: 802–811.
21. Weichert W, Kossakowski C, Harms A, *et al*. Proposal of a prognostically relevant grading scheme for pulmonary squamous cell carcinoma. *Eur Respir J* 2016; **47**: 938–946.
22. Shamji FM, Beauchamp G. Assessment of operability and resectability in lung cancer. *Thorac Surg Clin* 2021; **31**: 379–391.
23. Landis JR, Koch GG. The measurement of observer agreement for categorical data. *Biometrics* 1977; **33**: 159–174.
24. Bauer S, Dirksen U, Schildhaus HU. Systemic therapy of sarcomas: new biomarkers and therapeutic strategies. *Pathologe* 2019; **40**: 436–442.
25. Rakha EA, Reis-Filho JS, Baehner F, *et al*. Breast cancer prognostic classification in the molecular era: the role of histological grade. *Breast Cancer Res* 2010; **12**: 207.
26. Epstein JI, Egevad L, Amin MB, *et al*. The 2014 International Society of Urological Pathology (ISUP) Consensus Conference on Gleason Grading of Prostatic Carcinoma: definition of grading patterns and proposal for a new grading system. *Am J Surg Pathol* 2016; **40**: 244–252.
27. Steigen SE, Soland TM, Nginamau ES, *et al*. Grading of oral squamous cell carcinomas – intra and interrater agreeability: simpler is better? *J Oral Pathol Med* 2020; **49**: 630–635.
28. Brandwein-Gensler M, Teixeira MS, Lewis CM, *et al*. Oral squamous cell carcinoma: histologic risk assessment, but not margin status, is strongly predictive of local disease-free and overall survival. *Am J Surg Pathol* 2005; **29**: 167–178.
29. Bryne M, Koppang HS, Lilleng R, *et al*. Malignancy grading of the deep invasive margins of oral squamous cell carcinomas has high prognostic value. *J Pathol* 1992; **166**: 375–381.
30. Almangush A, Coletta RD, Bello IO, *et al*. A simple novel prognostic model for early stage oral tongue cancer. *Int J Oral Maxillofac Surg* 2015; **44**: 143–150.

31. Karpathiou G, Vieville M, Gavid M, *et al*. Prognostic significance of tumor budding, tumor-stroma ratio, cell nests size, and stroma type in laryngeal and pharyngeal squamous cell carcinomas. *Head Neck* 2019; **41**: 1918–1927.
32. Boxberg M, Bollwein C, Johrens K, *et al*. Novel prognostic histopathological grading system in oral squamous cell carcinoma based on tumour budding and cell nest size shows high interobserver and intraobserver concordance. *J Clin Pathol* 2019; **72**: 285–294.
33. Chouat E, Zehani A, Chelly I, *et al*. Tumor budding is a prognostic factor linked to epithelial mesenchymal transition in pancreatic ductal adenocarcinoma. Study report and literature review. *Pancreatology* 2018; **18**: 79–84.
34. Grigore AD, Jolly MK, Jia D, *et al*. Tumor budding: the name is EMT. Partial EMT. *J Clin Med* 2016; **5**: 51.
35. Thompson JC, Hwang WT, Davis C, *et al*. Gene signatures of tumor inflammation and epithelial-to-mesenchymal transition (EMT) predict responses to immune checkpoint blockade in lung cancer with high accuracy. *Lung Cancer* 2020; **139**: 1–8.
36. Boxberg M, Leising L, Steiger K, *et al*. Composition and clinical impact of the immunologic tumor microenvironment in oral squamous cell carcinoma. *J Immunol* 2019; **202**: 278–291.

SUPPLEMENTARY MATERIAL ONLINE

Figure S1. (A–C) Survival impact of tumour budding and (D–F) cell nest size in the Munich cohort

Figure S2. (A–C) Survival impact of tumour budding and (D–F) cell nest size in the Heidelberg cohort